Research Article

Jingdong Feng, Ziru Li, and Xiuyan Wang*

Two novel lead(II) coordination complexes incorporating phenanthroline derivate: Synthesis and characterization

https://doi.org/10.1515/mgmc-2022-8045 received December 29, 2022; accepted May 23, 2023

Abstract: Two lead(II) coordination complexes with 2-(4-fluoro-phenyl)-1H-imidazo[4,5-f][1,10]phenanthroline formulated as [Pb(L)₂(tlba)₂)] (1) and [Pb(L)(dpea)]₂ (2) (HTLBA = 2,3,4,5-tetrachlorobenzoic acid, H₂dpea = diphenic acid) were synthesized under hydrothermal conditions. In 1, the neighboring [Pb(L)₂(tlba)₂)] molecules formed into a two-dimensional (2D) layer structure with C–Cl··· π interactions and N–H···O hydrogen bond interactions. For 2, Pb1 and Pb1ⁱ ions are connected by four carboxylate groups from two dpea anions to yield a binuclear unit. Two L ligands are situated in two flanks of the dimer. The L ligands from dimers in the vicinity pile up by two π – π interactions to form a 2D supramolecular structure. Moreover, PXRD of 2 was also studied.

Keywords: lead(II), coordination complex, $C-Cl\cdots\pi$ interaction, $\pi-\pi$ interaction

1 Introduction

Coordination complexes are crystalline solids that can be self-assembled from metal centers and organic ligands and have attracted much attention from chemical researcher for their promising applications in catalysis (Sahoo and Sarma, 2022; Zheng et al., 2021), magnetism (Zhong et al., 2022), luminescence (Islam et al., 2021; Xu et al., 2022),

* Corresponding author: Xiuyan Wang, Key Laboratory of Preparation and Applications of Environmental Friendly Materials, Jilin Normal University, Ministry of Education, Changchun 130103, China; Department of Chemistry, Jilin Normal University, Siping 136000, China, e-mail: wangxiuyanjlnu2004@163.com

Jingdong Feng, Ziru Li: Key Laboratory of Preparation and Applications of Environmental Friendly Materials, Jilin Normal University, Ministry of Education, Changchun 130103, China; Department of Chemistry, Jilin Normal University, Siping 136000, China

biomedical applications (Chen and Wu, 2018), etc. Because the architecture of coordination complexes would be easily impacted by some conditions such as metal centers (Koksharova et al., 2023), nitrogen-containing ligands, carboxylate ligands (Song et al., 2020), and reaction conditions (Kharlamova et al., 2019). Therefore, selecting an appropriate organic ligand and adopting a befitting construction method can help us to obtain expectant coordination complexes (Wang et al., 2018). Nitrogen-containing ligands have shown outstanding coordination properties (Hou et al., 2014; Zhao et al., 2019) and multiple coordination modes (Leng et al., 2016) in past experiments. For example, 2-(4-fluoro-phenyl)-1*H*-imidazo[4,5-*f*][1,10]phenanthroline is a rigid ligand that can readily form hydrogen-bonding interactions and is an excellent composition for making up supramolecular architectures (Wang et al., 2019). Besides, carboxylate ligands play a significant role in the design and construction of various coordination complexes, and different carboxylate ligands can make the coordination complexes show different structures (Song et al., 2021; Su et al., 2022; Wang et al., 2016).

In this article, the coordination complexes were $[Pb(L)_2(tlba)_2]$ (1) and $[Pb(L)(dpea)]_2$ (2) (Htlba = 2,3,4,5-tetrachlorobenzoic acid, H_2 dpea = diphenic acid) and have been synthesized by hydrothermal methods and characterized.

2 Results and discussion

2.1 Structural analysis

Complex **1** crystallizes in the monoclinic space group C2/c with an independent Pb(II) ion, two L ligands, and two tlba anions. Each Pb(II) is mainly coordinated by four N atoms (from two chelating L ligands) and two oxygen atoms (O(1) and O(1ⁱ)) from two tlba anions (Pb(1)–O(1) = 2.613(5) Å) in a twisted [PbN₄O₂] octahedral geometry (Figure 1 and Table 1).

2 — Jingdong Feng et al. DE GRUYTER

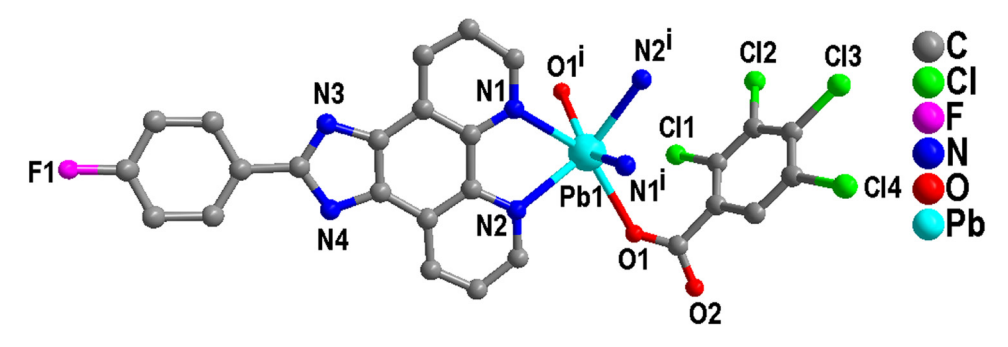


Figure 1: Coordination environment of the Pb(π) atom of **1** (symmetric code: i –x, y, –z + 1/2).

Table 1: Selected bond lengths (Å) and angles (°) for complexes 1 and 2

1			
Pb(1)-N(1)	2.560(5)	Pb(1)-O(1)	2.613(5)
Pb(1)-N(2)	2.572(5)		
N(1)-Pb(1)-N(1) ⁱ	84.3(2)	N(1)-Pb(1)-N(2) ⁱ	85.36(16)
$N(1)^{i}i-Pb(1)-N(2)^{i}$	64.40(16)	N(1)-Pb(1)-N(2)	64.40(16)
$N(1)^{i}-Pb(1)-N(2)$	85.36(16)	$N(2)^{i}-Pb(1)-N(2)$	139.5(2)
N(1)-Pb(1)-O(1)	144.56(19)	$N(1)^{i}-Pb(1)-O(1)$	78.69(17)
$N(2)^{i}-Pb(1)-O(1)$	113.93(14)	N(2)-Pb(1)-O(1)	83.28(16)
$N(1)-Pb(1)-O(1)^{i}$	78.69(17)	$N(1)^{i}-Pb(1)-O(1)^{i}$	144.56(19)
$N(2)^{i}-Pb(1)-O(1)^{i}$	83.28(16)	$N(2)-Pb(1)-O(1)^{i}$	113.94(14)
O(1)-Pb(1)-O(1) ⁱ	130.7(3)		
2			
Pb(1)-N(1)	2.665(5)	Pb(1)-O(2)	2.289(4)
Pb(1)-N(2)	2.525(4)	Pb(1)–O(3) ⁱ	2.666(4)
Pb(1)-O(4) ⁱ	2.347(4)		
$O(2)-Pb(1)-O(4)^{i}$	87.25(15)	O(2)-Pb(1)-N(2)	73.29(13)
$O(4)^{i}-Pb(1)-N(2)$	79.89(13)	O(2)-Pb(1)-N(1)	85.70(15)
$O(4)^{i}-Pb(1)-N(1)$	143.25(12)	N(2)-Pb(1)-N(1)	63.54(13)
$O(2)-Pb(1)-O(3)^{i}$	82.43(16)	$O(4)^{i}-Pb(1)-O(3)^{i}$	51.72(12)
$N(2)-Pb(1)-O(3)^{i}$	126.68(14)	$N(1)-Pb(1)-O(3)^{i}$	160.40(14)

Symmetry codes: 1: i -x, y, -z + 1/2; 2: i -x + 1, -y + 1, -z + 1.

The tlba anion chelates one Pb(II) with $\mu_I - \eta^1$ mode. It is noted that both the chlorine atoms involved in stacking lead to the formation of C(22)–Cl(1)··· π^1 (3.473(3) Å; π^1 : ring centroid of quinoline) and C(23)–Cl(2)··· π^2 (3.393(3) Å; π^2 : ring centroid of imidazole) interactions (Figure 2 and Table 2). And these C–Cl··· π interactions make the adjacent [Pb(L)₂(tlba)₂)] molecules to be formed into a one-dimensional supramolecular chain (Figure 3). Interestingly, there are N(4)–H(4)···O(2)ⁱⁱⁱ hydrogen bonds (symmetric code: iii -x + 1/2, y + 1/2, -z + 1/2), which extend the adjacent one-dimensional chains to extend into a two-dimensional (2D) supramolecular structure (Figure 4).

The asymmetric unit of **2** incorporates an independent 2Pb(n) ion and one L ligand, as well as one dpea anion. As shown in Figure 5, the Pb atom features a distorted [:PbN₂O₃]

octahedral geometry consisting of two N atoms (N(1), N(2)) from an L ligand and three oxygen atoms (O(2), O(3ⁱ), and O(4ⁱ)) from two dpea anions. The Pb–O distances are from 2.525(4) to 2.665(5) Å, and the Pb–N bond lengths are 2.289(4) and 2.666(4) Å. The basal plane of octahedral geometry is made up of two N and two O atoms, and the axial positions are comprised of the remaining O atom (O(2)) and the lone pair of electrons. Pb1 and Pb1ⁱ atoms are linked with four carboxylate groups from two μ_2 -dpea anions to generate a [Pb(L)(dpea)]₂ binuclear molecule. The Pb···Pb separation by two μ_2 -dpea anions is 6.701 Å. Two L ligands are situated in two flanks of the dimer (Figure 5).

The most remarkable feature of compound **2** is that there exist two types of π – π stacking interactions.

As depicted in Figure 6, the L ligands from dimers in the vicinity are paired through one type of strong $\pi{-}\pi$

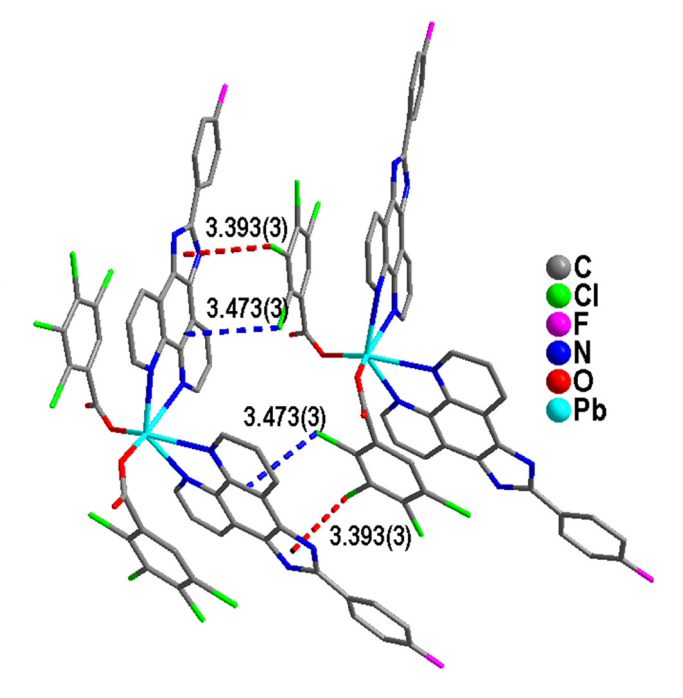


Figure 2: View of the C–Cl··· π interactions between tlba anions and L ligands.

Table 2: The chlorine interactions (Å, °) in complex 1

Υ-Χ…π	X…π (Å)	Y…π (Å)	y (°)	Y–X…π (°)	Symmetry code [#]
C(22)–Cl(1)···π ¹	3.473(3)	4.204(6)	13.07	102.36(18)	$-x$, $y - 1$, $-z + \frac{1}{2}$
$C(23)$ – $CI(2)$ ··· π^2	3.393(3)	3.726(7)	7.14	87.1(2)	$-x, y - 1, -z + \frac{1}{2}$

 π^1 : ring centroids of quinoline (N(1)/C(1)–C(6)/C(10)–C(11)); π^2 : ring centroids of imidazole (C(11)–C(12)/N(3)/C(13)/N(4)).

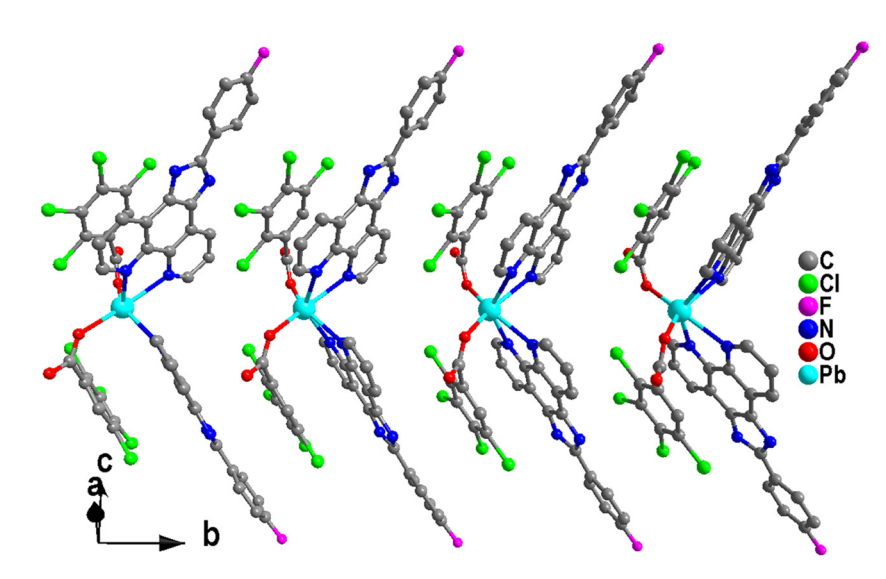


Figure 3: View of the 1D supramolecular chain of 1.

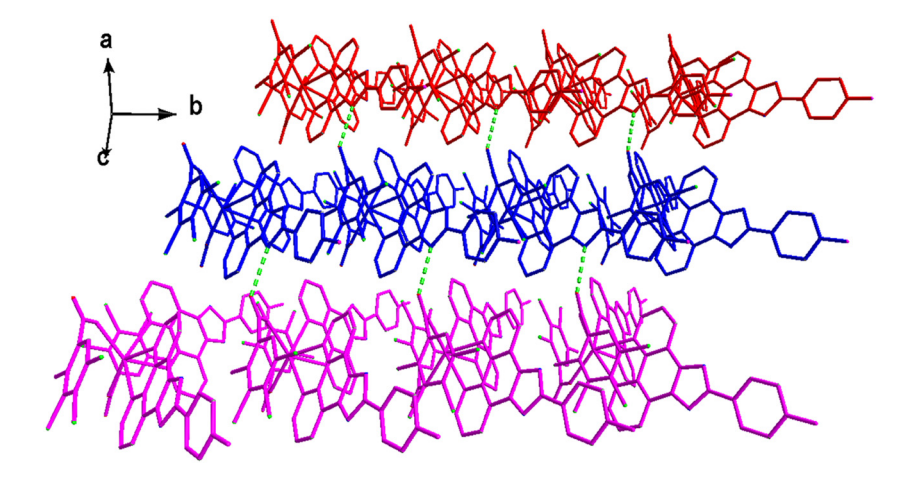


Figure 4: View of the 2D supramolecular layer structure of 1.

interactions (distance between ring centroids being ca. 3.401(2) Å, and dihedral angle of 0.00(11)°) to grow up to a one-dimensional supramolecular chain (Figure 7). More interestingly, neighboring 1D supramolecular chains are expanded to 2D supramolecular layer by the other types of π - π interactions between the two benzene rings of L ligands with the distance between ring centroids of 3.830(4) Å, a slippage distance of 1.866 Å, and a dihedral angle of 0.0(3)° (two benzene rings are composed of C(14)-C(19) and C(14)-C(19) at -1 - x, -y, -z; respectively) (Figure 8).

2.2 PXRD patterns

As seen in Figure 9, the diffraction peaks of 2 well correspond to the simulated powder X-ray diffraction (PXRD)

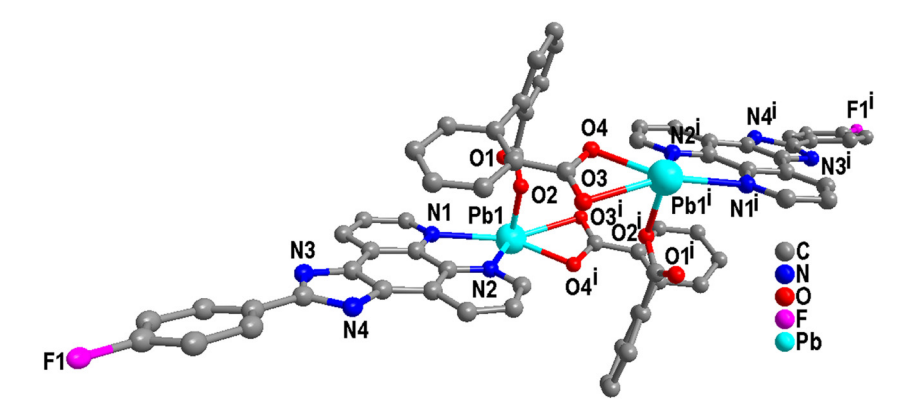


Figure 5: View of the dimeric structure of **2** (symmetric code: i -x + 1, -y + 1, -z + 1).

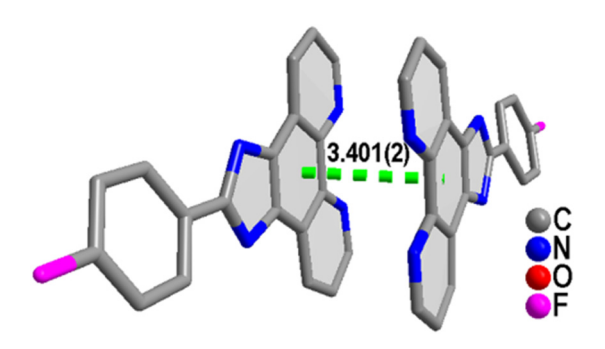


Figure 6: View of the π - π interactions between two L ligands of neighboring dimers.

from single crystal diffraction data, illustrating the phase purity of the yellow block crystals.

3 Conclusions

In conclusion, we have synthesized two novel coordination complexes based on Pb((II) via applying 2-(4-fuoro-phenyl)-1H-imidazo[4,5-f][1,10]phenanthroline and their structures were characterized. In **1**, the neighboring molecules are associated into a 2D supramolecular structure through the C–Cl··· π interactions as well as N–H···O hydrogen

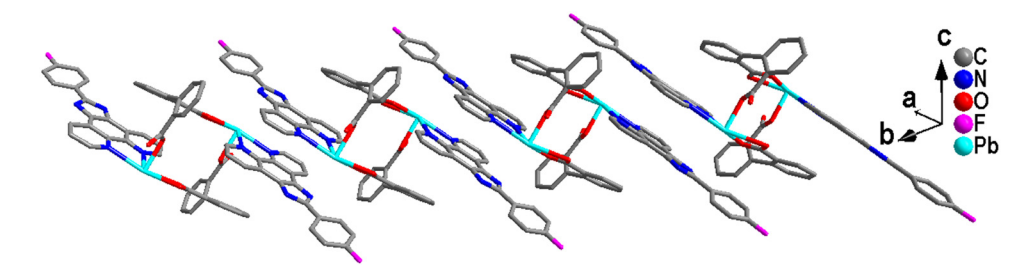


Figure 7: View of the 1D supramolecular chain of 2.

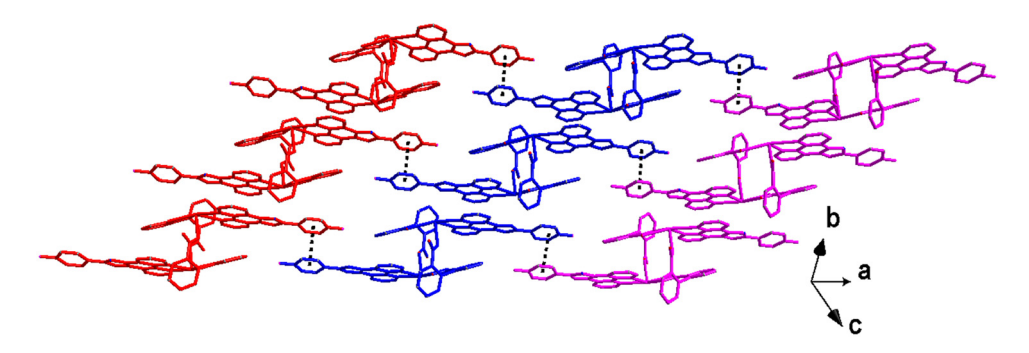


Figure 8: View of the 2D supramolecular layer of 2.

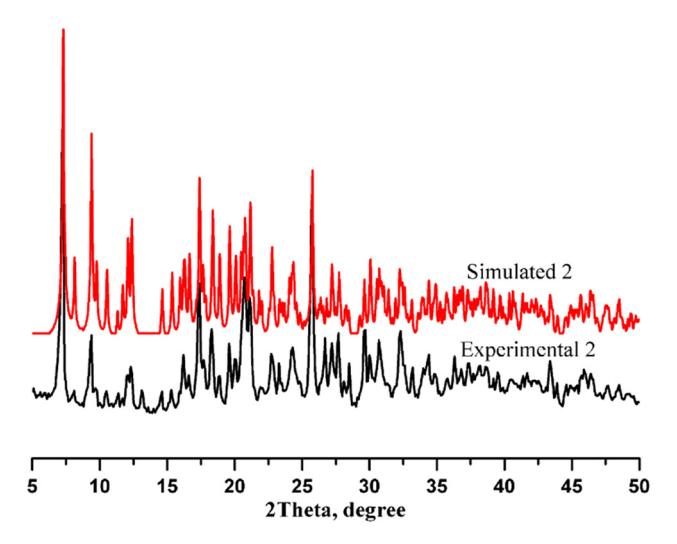


Figure 9: Experimental and simulated PXRD patterns of 2.

bonds. In **2**, the sideways L ligands from adjacent dipolymers are twined through two π - π stacking interactions to yield a 2D supramolecular layer. The different structures of the two complexes explain that carboxylic acid ligands play an essential part in the process of complex construction.

Table 3: Crystalline data and refinement parameters for complexes 1 and 2

Complex	1	1
Complex	1	2
Empirical formula	$C_{52}H_{24}C_{18}F_2N_8O_4Pb$	$C_{66}H_{38}F_2N_8O_8Pb_2$
Formula weight	1,353.58	1,523.42
Crystal system	Monoclinic	Triclinic
Space group	C2/c	P 1
a (Å)	18.177(6)	10.183(2)
b (Å)	8.5114(17)	11.790(2)
c (Å)	32.630(9)	12.137(2)
α (°)	90	93.70(3)
β (°)	105.34(3)	90.32(3)
y (°)	90	112.58(3)
Volume (ų)	4,868(2)	1,341.8(5)
Z	4	1
$D_{\rm c}$ (g·cm ⁻³)	1.847	1.885
μ (mm ⁻¹)	3.971	6.342
F (000)	2,640	736
heta range (°)	2.987-25.009	3.366-25.009
Crystal size (mm)	0.281 × 0.145 × 0.102	0.257 × 0.185 × 0.151
Tot. reflections	4,248	4,681
Uniq. reflections, R _{int}	18,207, 0.1334	10,549, 0.0472
GOF on F ²	1.050	1.031
R_1 indices $[I > 2\sigma(I)]$	0.0577	0.0332
wR_2 indices (all data)	0.0899	0.0747
$\Delta \rho_{\rm min}$, $\Delta \rho_{\rm max}$ (e·Å ⁻³)	-1.873, 1.438	-0.665, 1.486
CCDC No.	2232961	2232962

Experimental

The L ligand was compounded according to the procedures recounted in the document (Kong et al., 2015). All other chemicals with the quality of reagent grade were purchased from the mercantile sources (Cangzhou Shengqiang Chemical Technology Co., Ltd, and Wuhan Canrong Biological Technology Co., Ltd, China). The C, H, and N elemental analyses were carried out on a Perkin-Elmer 2400 elemental analyzer (Perkin-Elmer, North Waltham, USA). All PXRD analyses were recorded with a Rigaku Dmax 2000 X-ray diffractometer (Rigaku, Japan).

Preparation of $[Pb(L)_2(tlba)_2]$ (1)

Pb(NO₃)₂ (132 mg, 0.4 mmol), L (125 mg, 0.4 mmol), and HTLBA (208 mg, 0.8 mmol) were dissolved in a mixture of solvents (8 mL of deionized water and 2 mL of anhydrous ethanol), and the mixed solvent was agitated for 0.5 h at indoor temperature. Then adjusted the pH value to 9.45 with NaOH. The mixed solvent was sealed up in a 20 mL Teflon-lined stainless steel autoclave and kept at 185°C for 96 h. The brown rodlike crystals were gained in 37% yield (based on Pb). Analytical found for $C_{52}H_{24}C_{18}F_2N_8O_4Pb$, calculated %: C, 46.14; H, 1.79; N, 8.28; found %: C, 45.61; H, 1.77; N, 8.19.

Preparation of [Pb(L)(dpea)]₂ (2)

Pb(NO₃)₂ (331 mg, 1.0 mmol), L (151 mg, 0.48 mmol) and H₂dpea (242 mg, 1.0 mmol) were dissolved in a mixture of solvents (7 mL of deionized water and 3 mL of anhydrous ethanol), and the mixed solvent was agitated for 0.5 h at indoor temperature. Then adjusted the pH value to 5.69 with NaOH. The mixed solvent was sealed up in a 20 mL Teflon-lined stainless steel autoclave and kept at 140°C for 144 h. Yellow block crystals were gained in 40% yield (based on Pb). Analytical found for $C_{66}H_{38}F_2N_8O_8Pb_2$, calculated %: C, 52.04; H, 2.51; N, 7.36; found %: C, 51.61; H, 2.47; N, 7.25.

X-ray crystallography

The single-crystal data **1–2** were measured on an in-house Bruker P4 diffractometer equipped with a SMART CCD at

296(2) K, with graphite-monochromatized Mo- $K\alpha$ radiation (λ = 0.71073 Å) at room temperature. All the structures used SIR2014 to solve by direct methods (Burla et al., 2015) and ameliorated on F^2 by full-matrix least-squares techniques using the SHELXL2018/3 program (Sheldrick, 2015). The hydrogen atoms were geometrically placed in the computed positons and deemed to be riding. The non-hydrogen atoms were refined anisotropically and located. Crystallographic data for both complexes are presented in Table 3. Table 1 is the selected bond lengths and angles for complexes 1 and 2. Crystallographic data for the crystalline material have been deposited with the Cambridge Crystallographic Data Centre (CCDC), and the CCDC numbers are 2232961 and 2232962.

Funding information: The authors state that no funding is involved.

Author contributions: Jingdong Feng: writing – original draft, experimental work; Ziru Li: writing – original draft, conceptualization; Xiuyan Wang: software; data curation, experimental work.

Conflict of interest: The authors state no conflict of interest.

Data availability statement: All data generated or analyzed during this study are included in this published article.

References

- Burla M.C., Caliandro R., Carrozzini B., Cascarano G. L., Cuocci C., Giacovazzo C., et al., Crystal structure determination and refinement via SIR2014. J. Appl. Cryst., 2015, 48, 306–309. doi: 10.1107/S1600576715001132.
- Chen W., Wu C.S., Synthesis, functionalization, and applications of metal–organic frameworks in biomedicine. Dalton Trans., 2018, 47(7), 2114–2133. doi: 10.1039/c7dt04116k.
- Hou S.S., Tan J.B., Lian Z.Y., Zeng D.W., Huang T.L., Huang B.R., et al., Construction of three new mixed-ligand Zn(II) coordination polymers based on nitrogen-containing heterotopic ligands and carboxylate co-ligands. Inorg. Chem. Commun., 2014, 47, 112–118. doi: 10.1016/j.inoche.2014.07.002.
- Islam M.J., Kitagawa Y., Tsurui M., Hasegawa Y., Strong circularly polarized luminescence of mixed lanthanide coordination polymers with control of 4f electronic structures. Dalton Trans., 2021, 50(16), 5433–5436. doi: 10.1039/d1dt00519q.
- Koksharova T., Slyvka Y., Savchenko O., Mandzii T., Smola S., 5-Sulfosalicylato Cu(II), Zn(II) and Ni(II) coordination compounds with benzohydrazide: Synthesis, structure and luminescent properties. J. Mol. Struct., 2023, 1271, 133980. doi: 10.1016/j.molstruc.2022.133980.
- Kharlamova A.D., Abel A.S., Averin A.D., Beletskaya I.P., *N,N*-di(pyridin-2-yl)quinolin-6-amine: synthesis and coordination properties. Russ. Chem. B., 2019, 68(3), 597–600. doi: 10.1007/s11172-019-2460-0.

- Kong Z.G., Wang W., Zhang S.Q., Zhao F.W., Wang X.Y., Synthesis, crystal structure, physical properties and theoretical calculations of a new one-dimensional Ni(II) coordination polymer constructed by 1,10-phenanthroline derivative ligand and sulfate. J. Inorg. Organomet. P., 2015, 25(6), 1441–1447. doi: 10.1007/s10904-015-0257-7.
- Leng W.G., Peng Y.S., Zhang J.Q., Lu H., Feng X., Ge R.L., et al., Sophisticated design of covalent organic frameworks with controllable bimetallic docking for a cascade reaction. Chem Eur J., 2016, 22(27), 9087–9091. doi: 10.1002/chem.201601334.
- Sheldrick G.M., Crystal structure refinement with SHELXL. Acta Cryst., 2015, C71, 3–8. doi: 10.1107/S2053229614024218.
- Sahoo S., Sarma D., Synthesis, structure, and heterogeneous catalysis of a series of structurally diverse coordination polymers based on 5-nitroisophthalate. Cryst. Growth Des., 2022, 22(9), 5645–5657. doi: 10.1021/acs.cqd.2c00737.
- Song J., Duan B.F., Lu J.F., Ge H.G., Three new lanthanide coordination polymers constructed from 2,6-Bis(pyrazin-2-yl)pyridine-4-carboxy-late: syntheses, structures and luminescence. Chin. J. Struct Chem., 2020, 39(4), 793–800. doi: 10.14102/j.cnki.0254-5861.2011-2393.
- Song Y., Yan Y., Zhang H., Wang X.Y., Synthesis and structural characterization of a novel 2D supramolecular lead coordination polymer with phenanthroline derivate and adipic acid. Main. Group. Met. Chem., 2021, 44, 239–242. doi: 10.1515/mgmc-2021-0025.
- Su B.H., Shi Y.H., Peng X.H., Kong Z.G., Chang L.M., A new cadmium(II) coordination polymer with 1,4-cyclohexanedicarboxylate acid and phenanthroline derivate: synthesis and crystal structure. Main. Group. Met. Chem., 2022, 45, 208–212. doi: 10.1515/mgmc-2022-0020.
- Wang X.C., Chen Y., Yuan H., Yang Q., Zeng X.S., Qiu H.J., et al., Coordination polymers with 2D-3D interdigitated arrays based on 5-(4-(1H-1,2,4-Triazol-1-yl)phenyl)-1H-tetrazole: syntheses, structures, and properties. Z. Anorg. Allg. Chem., 2016, 642(11–12), 724–729. doi: 10.1002/zaac.201600120.
- Wang X.Y., Li C., Zou C.K., Kan R.F., Zhang X.X., Xu Z.L., A new Co(II) coordination polymer based on a flexible 1,4-cyclohexanedicar-boxylic acid: synthesis, structure and thermal behavior. Chin. J. Struct Chem., 2019, 38(12), 2155–2160. doi: 10.14102/j.cnki.0254-5861.2011-2482.
- Wang S.P., Liu J., Zhao H.M., Guo Z.F., Xing H.Z., Gao Y., Electrically conductive coordination polymer for highly selective chemiresistive sensing of volatile amines. Inorg. Chem., 2018, 57(2), 541–544. doi: 10.1021/acs.inorgchem.7b02464.
- Xu M.M., Lu H.J., Wang C.H., Qiu J., Zheng Z.F., Guo X.F., et al., Enhancing photosensitivity via the assembly of a uranyl coordination polymer. Chem. Commun., 2022, 58(67), 9389–9392. doi: 10.1039/ d2cc02985e.
- Zhao L., Liu X., Zhao C.J., Meng L.S., Synthesis and properties of interspersed structure complexes prepared from 4,4′-(phenylazanediyl)-dibenzoic acid with rigid and semi-rigid nitrogen-containing ligands. J. Mol. Struct., 2019, 1180, 547–555. doi: 10.1016/j.molstruc. 2018.12.026.
- Zhong X., Hu J.J., Yao S.L., Zhang R.J., Wang J.J., Cai D.G., et al., Gd (III)-Based inorganic polymers, metal-organic frameworks and coordination polymers for magnetic refrigeration. CrystengComm., 2022, 24(13), 2370–2382. doi: 10.1039/d1ce01633d.
- Zheng S.J., Pan J.P., Wang J.H., Liu S., Zhou T.T., Wang L., et al., Ag(I) pyridine-amidoxime complex as the catalysis activity domain for the rapid hydrolysis of organothiophosphate-based nerve agents: mechanistic evaluation and application. Acs Appl. Mater. Interface., 2021, 13(29), 34428–34437. doi: 10.1021/acsami.1c09003.